

Tanford, C. (1962), *Adv. Protein Chem.* 17, 69.  
 Vijai, K. K., and Foster, J. F. (1967), *Biochemistry* 6, 1152.  
 Wallevik, K. (1973), *J. Biol. Chem.* 248, 2650.  
 Williams, E. J., and Foster, J. F. (1960), *J. Am. Chem. Soc.* 82, 3741.

Woessner, D. E. (1962), *J. Chem. Phys.* 37, 647.  
 Zeppezauer, M., Lindman, B., Forsén, S., and Lindqvist, I. (1969), *Biochem. Biophys. Res. Commun.* 37, 137.  
 Zurawski, V. R., Jr., Kohr, W. J., and Foster, J. F. (1975), *Biochemistry* 14, 5579.

## Electronic and Resonance Raman Spectra of Iron(III) Complexes of Enterobactin, Catechol, and *N*-Methyl-2,3-dihydroxybenzamide<sup>†</sup>

Simon Salama, John D. Stong, J. B. Neilands, and Thomas G. Spiro\*

**ABSTRACT:** Resonance Raman electronic absorption and circular dichroism spectra and pH titration curves are reported for the trivalent ferric complexes of enterobactin, catechol, and *N*-methyl-2,3-dihydroxybenzamide (MDHB). The spectral signatures of the enterobactin and MDHB complexes are virtually identical and differ from those of the catechol complex in ways that reflect the influence of the amide group

on the electronic structure. Excitation in either the visible charge-transfer bands or the near-ultraviolet  $\pi$ - $\pi^*$  bands enhances Raman bands associated with benzene ring modes, although the relative enhancements differ markedly in the two regions. The data strongly support a structural model in which iron is bound exclusively to the phenolate oxygen atoms in all three complexes.

**B**lood diseases such as sickle cell anemia and  $\beta$ -thalassemia major are treatable only by transfusion therapy on a continued basis. Virtually all the iron administered as erythrocytes is retained and accumulated in the liver, heart and pancreas. Lacking an effective means of iron secretion, these tissues are subject to progressive fibrotic changes resulting in organ failure and death (Walker & Williams, 1974). Hence, an active interest is being taken in low molecular weight compounds capable of sequestering iron and rendering it in a form excretable by the body. Prime candidates are the bacterial iron transport chelators, which include desferrioxamine (Barry et al., 1974) and rhodotorulic acid (Grady et al., 1976). Rather high toxicity together with the required mode of administration (daily intramuscular injections) render these compounds less than ideal (Barry et al., 1974; Grady et al., 1976; Hwang & Brown, 1964). Another chelator, enterobactin, has received considerable attention (Smith, 1964; Gerwitz et al., 1965). This cyclic ester trimer of 2,3-dihydroxybenzoyl-1-serine (see Figure 1) is secreted by *Escherichia coli*, *Salmonella typhimurium*, and many other bacteria, and is 100 times more effective in sequestering iron and aiding in its transport than its monomer (Brot et al., 1966; O'Brien, 1966). In an effort to elucidate the structure and mode of iron binding in this complex we present here detailed spectroscopic studies of ferric enterobactin, together with two proposed model compounds, ferric tris(catecholate), first suggested by Webb and co-workers (Anderson et al., 1976), and a new complex, ferric tris(*N*-methyl-2,3-dihydroxybenzamide) (MDHB).<sup>1</sup>

### Experimental Section

Enterobactin was obtained as previously described (Llinas et al., 1973). The ferric complex was prepared by extracting the ligand from ethyl acetate into a suspension of ferric chloride, the pH of which was maintained at 7.5 by the addition of 1 M NaOH. The dark red-brown layer containing the complex was then centrifuged and filtered. The ligand *N*-methyl-2,3-dihydroxybenzamide was prepared from the acid chloride of 2,3-dihydroxybenzamide and methylamine. Five grams of the free acid was suspended in 25 mL of thionyl chloride purified by distillation from quinoline, followed by distillation from linseed oil. To this suspension was added 0.4 mL of dry dimethylformamide, and the mixture was stirred overnight under a gentle stream of nitrogen. During this time the acid chloride formed and dissolved in the excess thionyl chloride. The thionyl chloride was removed by distillation under reduced pressure, and the residue was washed with dry benzene which was also removed by vacuum distillation. The crude acid chloride was recrystallized from dry acetone. One gram of the purified acid chloride was dissolved in 50 mL of dry acetone. This solution was added dropwise over a 30-min period to a stirred 40% aqueous solution of methylamine. Argon was vigorously bubbled through the amine solution for 15 min prior to, and during, the addition of the acid chloride, and for 15 min thereafter. The solution was then cautiously adjusted to pH 5.5 with concentrated HCl, chilled to 0 °C and extracted twice with 1-volume portions of ether. The ether fractions were pooled, dried over anhydrous sodium sulfate, filtered, and stripped to dryness under reduced pressure. The crude amide was recrystallized from acetone-water. Anal. Calcd for  $C_8H_9NO_3 \cdot H_2O$ : C, 51.26; H, 5.92; N, 7.25. Found: C, 51.70; H, 5.23; N, 6.46. The ferric complex of this ligand was prepared in a manner similar to that of enterobactin, or by addition of a standardized solution of ferric chloride to a known quantity of the ligand. Crystalline ferric tris(catecholate) was a generous gift of Dr. John Webb.

Electronic absorption spectra were obtained with a Cary 118

<sup>†</sup> From the Department of Chemistry, Princeton University, Princeton, New Jersey 08540 (S.S., J.D.S., and T.G.S.), and the Department of Biochemistry, University of California, Berkeley, California (J.B.N.). Received February 27, 1978. The authors (S.S., J.D.S., and T.G.S.) gratefully acknowledge National Institutes of Health Grant GM13498, which supported this work.

<sup>1</sup> Abbreviations used: MDHB, *N*-methyl-2,3-dihydroxybenzamide; CD, circular dichroism; NMR, nuclear magnetic resonance; RR, resonance Raman.

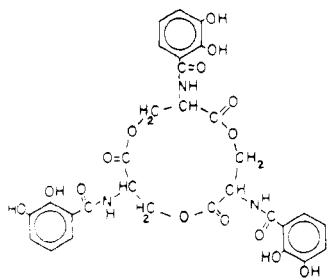


FIGURE 1: Structure of enterobactin.

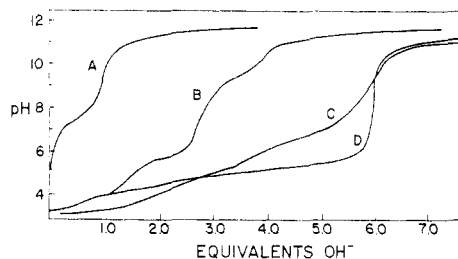


FIGURE 2: Proton titration curves. (A) MDHB; (B) ferric chloride-catechol, 1:3; (C) ferric chloride-MDHB, 1:3; (D) ferric enterobactin.

spectrophotometer, and CD spectra were obtained with a Jasco Model 20 automatic scanning spectropolarimeter. Raman spectra were obtained using a Spectra-Physics 170 Ar<sup>+</sup> laser and a Spex 1401 double monochromator with photon counting electronics. The UV laser lines were separated with a monochromator designed by Dr. James Nestor. Proton titrations were carried out using a Radiometer Model 26 pH meter and a Radiometer micro combination electrode. Additions of acid or base were made with a Micro-Metrics syringe and syringe buret. Nitrogen wetted with electrolyte (0.1 M KCl) was passed over the gently stirred samples throughout the titrations.

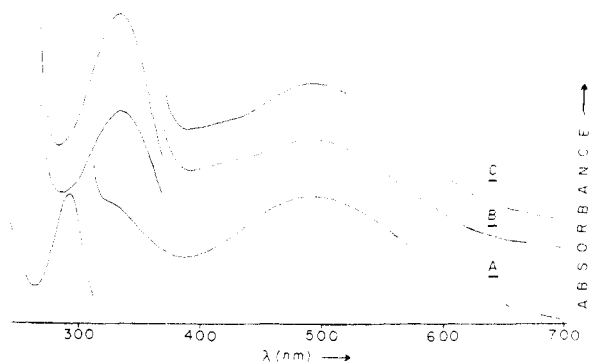
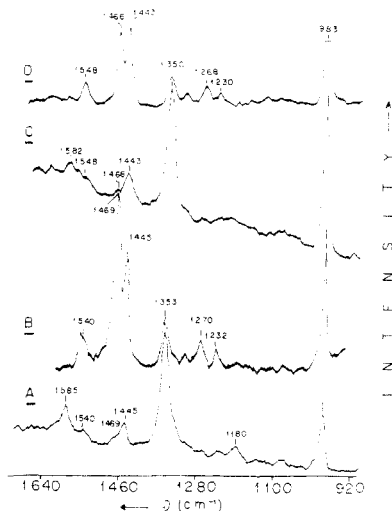
### Results and Discussion

Figure 2 shows pH titration curves for a 3:1 mixture of MDHB and catechol and ferric chloride and for free MDHB. Ferric enterobactin is also shown. The MDHB curve is consistent with the published  $pK_a$  values, 7.50 and 11.20, for the two hydroxyl groups. The ferric complex of MDHB and catechol each form with the release of six protons, as does ferric enterobactin. As seen in the titration curves (Figure 2) the model complexes exhibit lower  $pK_a$  values than ferric enterobactin up to about 2.5 proton equivalents. This implies a steric constraint imposed upon initial formation of the enterobactin complex. Subsequently, however, the enterobactin complex displays a more facile release of protons, reflecting a pronounced chelate effect. The sharpness of the endpoint for ferric enterobactin also demonstrates this enhanced stability, so that at pH 7.4 ferric enterobactin is virtually completely formed. The complex of MDHB, on the other hand, is only about 80% formed. Although the ferric tris(catecholate) titration curve roughly parallels the curve for the ferric chloride-MDHB mixture, the former displays lower stability, as expected from the higher  $pK_a$  values of catechol (see Table I). During the titration of the first four protons of the model complexes below pH 6.0, a blue-purple solution is formed, displaying a broad absorption band around 560 nm. This band is similar to that of the ferric catecholate dimer complex characterized by Anderson et al. (1976). Titration of the last two protons, which is associated with a plateau defining a  $pK_a$  of about 7.0, produces a reddish brown solution.

TABLE I:  $pK_a$  Values of Hydroxyl Groups in Different Phenolate Type Compounds.<sup>a</sup>

compound	$pK_1$	$pK_2$
phenol	10.50	
catechol	9.48	12.08
1,4-dihydroxybenzene	9.96	11.39
salicylamide	8.37	
<i>N</i> -Me-2,3-DHB-amide	7.50	11.20

<sup>a</sup> From Rappoport (1967).

FIGURE 3: Electronic absorption spectra. (A) Ferric tris(catecholate); (B) ferric enterobactin; (C) Fe(MDHB)<sub>3</sub><sup>3-</sup>.FIGURE 4: RR spectra of (A and B) ferric enterobactin ( $10^{-3}$  M) and (C and D) Fe(MDHB)<sub>3</sub><sup>3-</sup> complexes ( $10^{-3}$  M). Conditions: (A and C) 363.8 nm laser excitation, 200 mW, spectral slit 15 cm<sup>-1</sup>, time constant 5 s, scanning speed 0.5 cm<sup>-1</sup>/s, sensitivity  $2 \times 10^3$  counts per s; (B and D) 5145 Å excitation, 200 mW, spectral slit 12 cm<sup>-1</sup>, time constant 5 s, scanning speed 0.5 cm<sup>-1</sup>/s, sensitivity  $10^3$  counts per s.

The absorption spectrum of the MDHB complex with six protons ionized, which we write as Fe(MDHB)<sub>3</sub><sup>3-</sup>, is nearly the same as that of ferric enterobactin, as shown in Figure 3. For ferric enterobactin,  $\lambda_{max} \approx 500$  nm ( $\epsilon = 3.2 \times 10^3$  M<sup>-1</sup> cm<sup>-1</sup>), and for Fe(MDHB)<sub>3</sub><sup>3-</sup>  $\lambda_{max} \approx 500$  nm ( $\epsilon = 1.9 \times 10^3$  M<sup>-1</sup> cm<sup>-1</sup>). Moreover, the resonance Raman spectra are very nearly the same, as shown in Figure 4. The spectral similarities are so faithful that they leave no room to doubt that the two chromophores have the same chemical structure. This structure is almost certainly iron coordinated by two phenolate oxygen atoms from each of the three ring systems with no involvement of amide nitrogen in the iron coordination sphere (referred to as structure 1). The only alternative would be iron coordinated by a single phenolate oxygen and deprotonated amide nitrogen

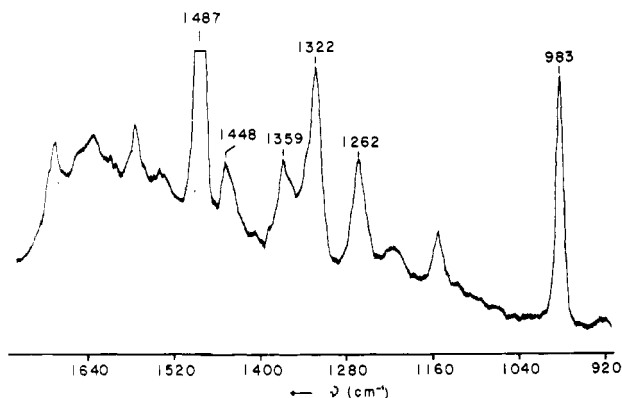


FIGURE 5: RR spectrum of ferric tris(catecholate) complex ( $2 \times 10^{-3}$  M) with 496.5 nm laser excitation. Conditions: laser power 200 mW, spectral slit  $12 \text{ cm}^{-1}$ , time constant 5 s, scanning speed  $0.5 \text{ cm}^{-1}/\text{s}$ , sensitivity 500 counts per s.

from each of the three ring systems (referred to as structure **2**). However, **1** is much more likely, for the following reasons. (1) The tris(catecholate) complex, analogous to **1**, has a similar electronic absorption spectrum, as shown in Figure 3; the resonance Raman spectrum, Figure 5, is also fairly similar. The resemblances are not as close as between  $\text{Fe}(\text{MDHB})_3^{3-}$  and ferric enterobactin, but the differences are plausibly connected to the influence of an uncoordinated amide group (see below). (2) The phenolic protons are more acidic than the amide proton. The  $\text{p}K_a$ s listed in Table I demonstrate this point. The phenol  $\text{p}K_a$ , 10.50, is split to 9.96 and 11.39 in 1,4-dihydroxybenzene. In catechol an extra splitting, to 9.48 and 12.08, can be attributed to the stabilization of the monoprotonated species by the internal hydrogen bond between the orthophenolate oxygen atoms. Ring substitution by an amide functionality decreases the  $\text{p}K_a$ , as seen for salicylamide (8.37), due to its electron-withdrawing character. There is no evidence, however, that the amide protons of salicylamide ionize at a measurable pH. The  $\text{p}K_a$  values of MDHB are consistent with those expected for catechol after the introduction of an amide group ortho to one of the oxygen atoms.

If **2** were an accessible structure, then it should be possible to form an analogous tris(chelate) with salicylamide. A titration of ferric chloride-salicylamide (1:3) was also performed (not shown). It was found that two protons per iron atom were released in the development of a chromophore with an absorption at 525 nm, characteristic of iron-salicylate dimers (David & David, 1977). The proton titration curve showed the dissociation of two protons per iron below pH 5, followed by the release of a third proton ( $\text{p}K_a = 7.4$ ) which resulted in a brown precipitate. There was no indication of the dissociation of the amide proton. This implies a structure for the ferric salicylamide complex similar to that of the ferric salicylic acid dimer described by David & David (1977). Only weak interactions exist (if any) between the amide nitrogen (or carbonyl oxygen) and the iron. (3) Frequency shifts in RR spectra recorded in  $\text{D}_2\text{O}$  (see below) are attributable to exchange of the amide proton in **1**. If the structure were **2** instead, then the shifts would have to be attributed to proton exchange on the uncoordinated phenol group. This proton would be expected to be lost at high pH, however. The  $\text{p}K_a$  of the uncoordinated phenol would certainly be expected to be lower (via the polarization effects of  $\text{Fe}^{3+}$ ) than the second  $\text{p}K_a$  of free MDHB, 11.20. Yet the Raman deuteration shifts were observed to persist in solutions with a pH of 12. (4) The enterobactin complex with  $\text{Ga}^{3+}$  has been shown by NMR evidence to have

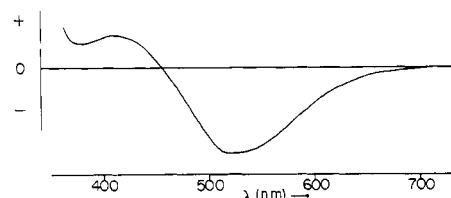


FIGURE 6: Circular dichroism spectrum of ferric enterobactin.

TABLE II: Raman Frequencies of Ferric Enterobactin and Its Model Complexes ( $\text{cm}^{-1}$ ).

ferric enter.		ferric 2,3-DHB-amide		ferric catechol <sup>a</sup>
$\text{H}_2\text{O}$	$\text{D}_2\text{O}$	$\text{H}_2\text{O}$	$\text{D}_2\text{O}$	$\text{H}_2\text{O}$
525	565	565	565	533
637	637			621
		650 (br)	650 (br)	
667	667			
				800
1180 (w)				1154
1232	1210	1238	1220	1216
1270	1275	1269	1274	1262
				1322
1353	1340	1350	1337	1359
1445	1448	1443	1444	1448
1469	1482	1466	1480	1487
1540	1542	1548	1547	1572
1585	1585	1582	1582	

<sup>a</sup> No attempt to correlate between these frequencies and those of the other two compounds. The parallelism in the listing of these frequencies is only for clarity in the table.

structure **1** (Llinas et al., 1973) and it is reasonable to expect  $\text{Fe}^{3+}$  to bind similarly.

**Electronic Spectra.** The reddish brown colors of the ferric enterobactin, tris(MDHB) and tris(catecholate) complexes are due to a broad absorption band, centered at  $\sim 500 \text{ nm}$ . This is characteristic of phenolate bound to iron(III) (Brot et al., 1966; Gaber et al., 1974) and has been assigned to a phenolate  $\rightarrow \text{Fe}^{3+}$  charge transfer transition. The band is symmetric for the catecholate complex, but both MDHB and enterobactin show a shoulder at  $\sim 412 \text{ nm}$ . The presence of an extra transition at this wavelength is confirmed by the circular dichroism spectrum of  $\text{Fe}^{\text{III}}$  enterobactin, Figure 6, which shows a negative peak at 520 nm, and a positive one, of smaller amplitude at 412 nm. Both  $\text{Fe}(\text{MDHB})_3^{3-}$  and ferric tris(catecholate) displayed no significant optical activity, implying a lack of structural restraint in complex formation resulting in a mixture of enantiomers. The steric constraints imposed by the rigid ring structure of enterobactin, however, result in the formation of only one configuration, giving rise to the CD spectrum shown in Figure 6. The existence of two charge-transfer transitions, separated by  $\sim 5000 \text{ cm}^{-1}$ , probably reflects the involvement of the amide group in the aromatic conjugation. It would be expected to lower the  $\pi$  orbital energy on the ortho hydroxyl group, while its effect on the meta hydroxyl group is small.

A somewhat more intense band is observed at 290 nm for the catecholate complex and at 330 nm for the MDHB and enterobactin complexes (O'Brien & Gibson, 1970). These are assignable to aromatic  $\pi-\pi^*$  transitions, the positions shifting to longer wavelengths with increasing delocalization, via the amide group (Silverstein et al., 1974). Similar bands are observed for deprotonated catechol and MDHB. The catecholate complex also displays a shoulder at 330 nm. As in the case of a previously studied transferrin analogue (Gaber et al., 1974),

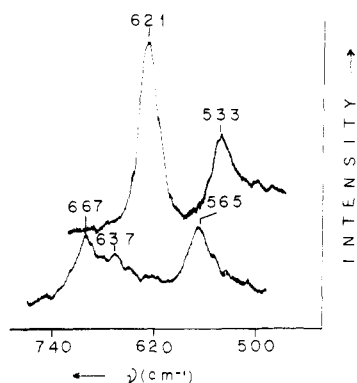


FIGURE 7: RR spectra of  $2 \times 10^{-3}$  M ferric Tris-catecholate (upper spectrum) and  $10^{-3}$  M ferric enterobactin using 514.5 nm laser excitation. Conditions: laser power 200 mW, spectral slit  $12 \text{ cm}^{-1}$ , time constant 5 s, scanning speed  $0.5 \text{ cm}^{-1}/\text{s}$ , sensitivity  $10^3$  counts per s.

the ferric catecholate bands at  $\sim 500$  and  $\sim 300$  nm can reasonably be assigned to two charge-transfer transitions, terminating on the  $d_{\pi}$  and  $d_{\sigma}$  Fe(III) orbitals, respectively, the separation ( $\sim 10\,000 \text{ cm}^{-1}$ ) being in the range expected for 10 Dq in octahedral Fe(III) complexes with oxygen ligands (Schlafer & Gliemann, 1969). For the MDHB and enterobactin complexes the  $d_{\sigma}$  charge transfer transitions (two are expected since two  $d_{\pi}$  transitions are observed in the visible region) are probably buried under the more intense  $\pi$ - $\pi^*$  band. The near-UV CD spectrum of the enterobactin complex (not shown) does show evidence of more than one transition in the 330-nm region.

**Resonance Raman Spectra.** The RR spectra of the complexes under study are dominated by bands in the region  $1000$ – $1600 \text{ cm}^{-1}$ , as shown in Figures 3 and 4 and catalogued in Table II. The band at  $1262$ – $1270 \text{ cm}^{-1}$  is expected to have a major contribution from phenolate C–O stretching. The remaining bands are attributable to skeletal modes of the substituted benzene ring. Thus the bands observed in the catecholate spectrum, Figure 5, at  $1572$ ,  $1487$ ,  $1448$ ,  $1359$ ,  $1322$ , and  $1154 \text{ cm}^{-1}$  can be identified with benzene modes 8a, 19b, 19a, 14, 3, and 15, respectively (Varsanyi & Szohe, 1969), which are known to fall at about these positions in ortho-disubstituted benzenes. With 496.5-nm excitation, the largest enhancement, and therefore the largest origin shift in the charge-transfer excited state, is observed for mode 19b,  $1487 \text{ cm}^{-1}$ , which has a large contribution from the stretching of the bond between the carbon atoms to which the two oxygen atoms are attached.

Essentially the same bands, with moderate frequency shifts and relative intensity changes, are seen for the enterobactin and MDHB complexes. No additional bands, attributable to the amide group, are observed. The lack of major amide contribution to the enhanced modes is confirmed by the  $\text{D}_2\text{O}$  shifts (Table II). None of these exceed  $22 \text{ cm}^{-1}$ , while modes localized on the amide group are expected to show larger shifts (Armendarez & Nakamoto, 1970).

Although the low-frequency RR spectra are weak, 514.5 nm excitation does bring out two bands of the catecholate complex, at  $621$  and  $533 \text{ cm}^{-1}$ , as shown in Figure 7. The  $621\text{-cm}^{-1}$  band may correspond to the lowest in-plane deformation mode of benzene, at  $606 \text{ cm}^{-1}$  (Varsanyi & Szoze, 1969). The  $533\text{-cm}^{-1}$  band is close to the chelate ring mode observed in  $\text{Fe}(\text{oxalate})_3^{3-}$  at  $528 \text{ cm}^{-1}$  (Nakamoto, 1970). Ferric enterobactin shows a similar mode at  $565 \text{ cm}^{-1}$  (Figure 7). The metal–oxygen stretch of  $\text{Fe}(\text{oxalate})_3^{3-}$  is found at  $366 \text{ cm}^{-1}$  (Nakamoto, 1970). No comparable band is found in the RR spectra of the catecholate, MDHB, or enterobactin complexes.

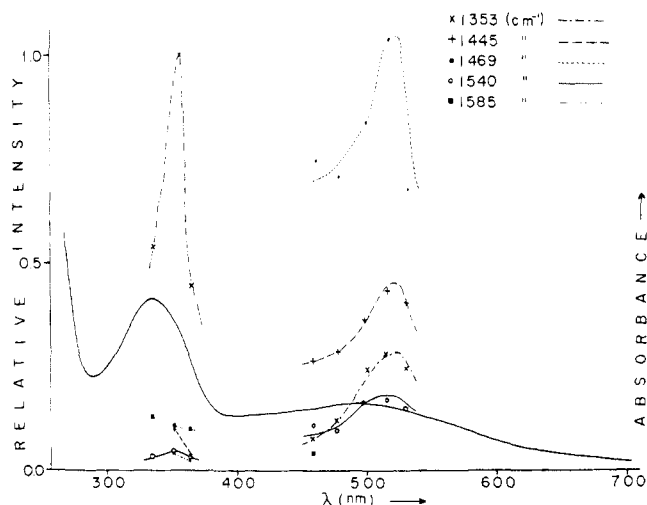


FIGURE 8: Excitation profile of ferric enterobactin high frequency modes. The scale of the profile in the UV region is five times that of the visible region.

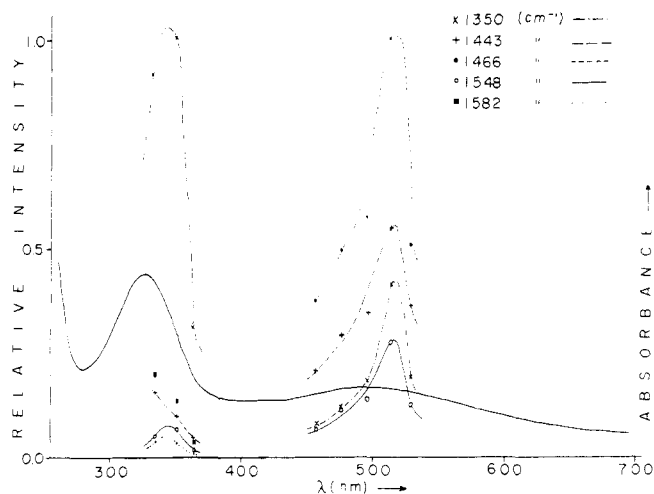


FIGURE 9: Excitation profile of  $\text{Fe}(\text{MDHB})^-$  modes in the high frequency region. The scale of the profile in the UV region is five times that of the visible region.

As in the case of transferrin and its analogue complex, for which no Fe–O modes could be located (Gaber et al., 1974), we interpret this result as reflecting an unchanged Fe–O bond length in the excited state, presumably because the terminal orbital of the charge-transfer transition is a  $d_{\pi}$  orbital on iron, and therefore nonbonding.

Figures 8 and 9 show excitation profiles for the enterobactins and MDHB complexes. In the visible region all bands maximize at  $19\,200 \text{ cm}^{-1}$  ( $520 \text{ nm}$ ) coincident with the negative peak in the ferric enterobactin CD spectrum (Figure 6). The profiles are skewed to the high-energy side, and, in the case of the MDHB complex, a definite shoulder can be seen  $\sim 1000 \text{ cm}^{-1}$  above the main peak. This is reminiscent of the situation found in transferrin, where all modes show a progression of excitation profile maximum with a spacing of  $1000 \text{ cm}^{-1}$  (Gaber et al., 1974). This was interpreted as the C–O frequency in the excited state, the maximum reflecting the dominance of the C–O bond-length change in the excited state distortion.

Excitation in the near-UV region did not produce good quality spectra for the catecholate complex, but did produce excellent spectra (Figure 4) for the enterobactin and MDHB

complexes, for which the Ar<sup>+</sup> UV lines, 363.8, 351.1, and 333.1 nm are in resonance with the  $\pi$ - $\pi^*$  transition. The intensity pattern is quite different from the spectra with visible excitation. One band, at 1350 cm<sup>-1</sup> is dominant. Its excitation profile, shown in Figures 8 and 9, peaks to the red of the absorption maximum. The 333.1-nm Ar<sup>+</sup> line is at the top of the absorption band, and the Raman intensity is definitely lower than at 351.1 nm. This behavior is reminiscent of the antiresonance phenomenon seen in transition-metal complexes where excitation profiles maximize to the red of ligand-field absorption bands, reflecting an interference between the weak resonance enhancement of the local forbidden state and the comparably strong preresonance enhancement of a higher-allowed transition (Stein et al., 1976; Zgierski, 1977; Korenowski et al., 1978). The same explanation may apply in the present instance, since the 330 nm  $\pi$ - $\pi^*$  transition, although moderately intense, is actually partly forbidden (Varsanyi & Szoke, 1969).

The 1466- and 1548-cm<sup>-1</sup> modes follow excitation profiles that are weaker, but similar in shape to the 1350-cm<sup>-1</sup> excitation profiles. On the other hand the intensities of the 1443- and 1582-cm<sup>-1</sup> modes increase monotonically with decreasing wavelength. They appear not to be resonant with the 330-nm transition but rather with the 243-nm transition.

#### Acknowledgments

We thank Dr. John Webb for the sample of ferric catecholate and Dr. Charles R. Hartzell for the use of the Jasco spectrophotometer and the kind loan of the Micrometrics titration equipment. Elemental analyses were performed by Eli-Lilly.

#### References

- Anderson, B. F., Buckingham, D. A., Robertson, G. B., Webb, J., Murray, K. S., & Clark, P. E. (1976) *Nature (London)* 262, 722.
- Armerdarez, P. X., & Nakamoto, K. (1966) *Inorg. Chem.* 5, 796.
- Barry, M., Flynn, D. M., Letsky, E. A., & Risdon, R. A. (1974) *Br. Med. J.* 1, 16.
- Brot, N., Goodwin, J., & Fales, H. (1966) *Biochem. Biophys. Res. Commun.* 25, 454.

- David, P. G., & David, F. (1977) *J. Coord. Chem.* 6, 211.
- Gaber, B. P., Miskowski, V., & Spiro, T. G. (1974) *J. Am. Chem. Soc.* 96, 6868.
- Gerwitz, N. R., Tendler, D., Lurinsky, G., & Wasserman, L. R. (1965) *N. Engl. J. Med.* 273, 95.
- Grady, R. W., Grazziano, J. H., Akers, H. A., & Cerami, A. (1976) *J. Pharmacol. Exp. Ther.* 196, 478.
- Hwang, Y. F., & Brown, E. B. (1964) *Arch. Intern. Med.* 114, 741.
- Korenowski, G. M., Ziegler, L. D., & Albrecht, A. C. (1978) *J. Chem. Phys.* 68, 1248.
- Llinas, M., Wilson, D. M., & Neilands, J. B. (1973) *Biochemistry* 12, 3836.
- Nakamoto, K. (1970) *Infrared Spectra of Inorganic and Coordination Compounds*, p 245, Wiley-Interscience, New York, N.Y.
- O'Brien, I. G., & Gibson, F. (1970) *Biochim. Biophys. Acta* 215, 393.
- O'Brien, I. G., Cox, G. B., & Gibson, F. (1969) *Biochim. Biophys. Acta* 177, 321.
- Pollack, J. R., & Neilands, J. B. (1970) *Biochem. Biophys. Res. Commun.* 38, 989.
- Rappoport, Z. (1967) *Handbook of Tables of Organic Compound Identification*, 3rd ed, Chemical Rubber Publishing Co., Cleveland, Ohio.
- Schlafer, H. L., & Gliemann, G. (1969) *Basic Principles of Ligand Field Theory*, p 78, Wiley-Interscience, New York, N.Y.
- Silverstein, R. M., Bassler, G. C., & Morrill, T. C. (1974) *Spectroscopic Identification of Organic Compounds*, Wiley, New York, N.Y.
- Smith, R. S. (1964) *Ann. N.Y. Acad. Sci.* 119, 776.
- Stein, P., Miskowski, V., Woodruff, W. H., Griffin, J. P., Werner, K. G., Gaber, B. P., & Spiro, T. G. (1976) *J. Chem. Phys.* 64, 2159.
- Varsanyi, G., & Szoke, S. (1969) *Vibrational Spectra of Benzene Derivatives*, p 71, Academic Press, New York, N.Y.
- Walker, R. J., & Williams, R. (1974) in *Iron in Biochemistry and Medicine* (Jacobs, A., & Worwood, M., Eds.) p. 596, Academic Press, New York, N.Y.
- Zgierski, M. Z. (1977) *J. Raman Spectrosc.* 6, 53.